

Quantum-well states in Cu/Co overlayers and sandwiches

P. van Gelderen

Institute for Theoretical Physics, University of Nijmegen, Toernooiveld, NL-6525 ED Nijmegen, The Netherlands

S. Crampin

School of Physics, University of Bath, BA2 7AY, United Kingdom

J. E. Inglesfield*

Institute for Theoretical Physics, University of Nijmegen, Toernooiveld, NL-6525 ED Nijmegen, The Netherlands

(Received 23 August 1995)

We report *ab initio* calculations of quantum-well states in Cu/Co(001) and Co/Cu(001) overlayers and in Co/Cu/Co(001) sandwiches. Overlayer states are found which coincide well with those previously identified in photoemission and inverse photoemission experiments. In Cu/Co and at energies overlapping with the substrate continuum, minority spin resonances are clearly identifiable. However, in the majority spin channel coupling to the substrate is strong enough to effectively destroy quantum-well features. In Co/Cu/Co(001) sandwiches discrete states are found at similar energies to those in overlayers of corresponding Cu thicknesses, but well defined resonance states are absent in both spin channels. There is no longer a strongly size-dependent electronic structure at the Fermi energy. We conclude care must be taken in extrapolating from the electronic structure of overlayer systems to that of other modulated structures.

I. INTRODUCTION

There has been recent interest in the electronic states in interlayer and overlayer systems built up from magnetic and nonmagnetic metals. This is because interlayer systems such as Co/Cu/Co show an exchange coupling between the Co layers through the Cu spacer layer which is oscillatory in the layer thickness. Two explanations (which both give the correct periods of the oscillation, e.g., for the Fe/Cr/Fe system¹) have been given for this behavior. The first, which is perturbative and valid for small moments, is based on the Ruderman-Kittel-Kasuya-Yosida (RKKY) oscillations through the spacer, whose period depends on Fermi surface parameters; the second is based on spin-split quantum-well states whose occupation depends on their energy and hence on the layer thickness. In this paper we shall study the properties of these states, in particular in the epitaxially grown overlayer systems of Co/Cu(001) and Cu/Co(001), and in the Co/Cu/Co(001) sandwich system.

In non-spin-polarized photoemission (PE) and inverse photoemission (IPE) experiments Ortega *et al.*^{2,3} have observed features, identified as quantum-well states, in several overlayer systems consisting of a nonmagnetic noble metal and a ferromagnetic material. The energy of these states depends on the overlayer thickness, and they are seen to cross the Fermi level E_F at regular intervals. Recently, two groups have reported spin-resolved PE experiments^{4,5} on Cu/Co(001) and have established that the states below E_F are spin polarized. Carbone *et al.*⁴ found the quantum-well levels to be split by about 0.20 eV, which is in good agreement with a recent *ab initio* calculation by Nordström *et al.*,⁶ who found a splitting of 0.16 eV for Cu overlayer states in the Cu/Co/Cu(001) system, where the Co thickness varied from 1 to 25 ML (monolayer). Both Carbone *et al.*⁴ and Garrison *et al.*⁵ found that the majority spin states give a much weaker

signal than the minority spin states. Indeed, Garrison *et al.*⁵ were not able to identify majority spin features at all. An interesting aspect of these results is that the period with which the quantum-well levels cross E_F equals the longer period of the oscillatory exchange coupling between layers of Co separated by an interlayer of variable thickness of Cu. From Fermi surface parameters this period is deduced to be 6 monolayers (ML),⁷ and experimentally it is found to be about 8 ML (Ref. 8) for [001] stacking. Jones *et al.*⁹ show that long oscillation periods could have contributions from quantum-well states. On the other hand, Mathon *et al.*¹⁰ have shown very recently that in their model the short period oscillation is dominant due to the existence of quantum-well states near the Cu Fermi surface neck in the ferromagnetic configuration. The contribution of quantum-well states to the longer period is negligible in this model. In this paper we report a study of the quantum-well states associated with various overlayers and sandwich systems constructed from stacked Cu and Co planes, and we discuss the relationship between them.

II. COMPUTATIONAL METHOD

We use the multiple scattering layer Korringa-Kohn-Rostoker (LKKR) electronic structure method,^{11,12} which is a generalization to systems with two-dimensional translational symmetry of conventional KKR theory.¹³ This Green function method is preeminently suitable for planar geometry since the solid is partitioned into layers of atoms. The scattering properties of each layer are calculated in a partial-wave basis set in which use is made of the two-dimensional translational symmetry, and the layers are then coupled together in a plane-wave basis set to form the complete system. With this method we are able to study overlayers, interlayers and surfaces, taking into account the full semi-infinite sub-

strate, thus modeling the experiments very accurately without any slab assumption. This is important when studying quantum well states in order to avoid any features originating from the discreteness of states in slab calculations. The method is very fast, though it suffers from the disadvantage that it is not full potential—instead we use the atomic sphere approximation (ASA) for the potentials. This hardly matters, we believe, in the closed packed metallic systems we study here. The electronic structure is calculated self-consistently within the local spin density approximation. The charge and spin density, together with other static properties of interest such as the local density of states (LDOS) are found from the Green function, which is calculated directly in this method.

In KKR, as in other scattering methods, the Green function of the solid is given by Dyson's equation

$$G = G_0 + G_0 T G_0, \quad (1)$$

where G_0 is the free particle Green function and T is the total scattering operator of the system, which sums up all scattering paths of an electron through the system (see, e.g., Gonis¹⁴). T has an expansion in site-labeled scattering-path operators $\tau^{\alpha\beta}$, where $\tau^{\alpha\beta}$ sums all scattering paths beginning and ending with scattering events at sites α and β , respectively:

$$T = \sum_{\alpha\beta} \tau^{\alpha\beta}. \quad (2)$$

The scattering path operators satisfy equations of motion,

$$\tau^{\alpha\beta} = t^\alpha \delta_{\alpha\beta} + t^\alpha \sum_{\gamma \neq \alpha} G_0^{\alpha\gamma} \tau^{\gamma\beta}, \quad (3)$$

in terms of the atomic scattering operator t^α and the intersite propagator $G_0^{\alpha\beta}$. This equation is solved within the angular momentum basis $L = (\ell, m)$.

For a bulk crystal, taking lattice Fourier transforms of Eq. (3) assuming identical potentials in each sphere (so $t^\alpha = t$ for all α), the Fourier transform of τ is obtained from a matrix inversion:

$$\tau(\mathbf{K}) = [t^{-1} - G(\mathbf{K})]^{-1}. \quad (4)$$

Both t and $G(\mathbf{K})$ (the KKR structure constants, the lattice Fourier transform of $G_0^{\alpha\beta}$) are functions of the electron energy E , but all the information about the structure is in $G(\mathbf{K})$ while all the information about the potential is carried by t . The band structure is given by the poles of the scattering matrix; at a given energy E the allowed wave vectors \mathbf{K} , if any, can be obtained from

$$\det[\tau(\mathbf{K})] = 0. \quad (5)$$

We use the LKKR method for systems lacking full translational periodicity, studying electronic properties layer by layer. We utilise translational periodicity within each layer, and project out the Green function about atoms in different layers. To do this, we introduce the operator $T^{\alpha\alpha}$ which sums all scattering events which neither begin nor end on site α ,

$$T^{\alpha\alpha} = \sum_{\substack{\beta \neq \alpha \\ \gamma \neq \alpha}} \tau^{\beta\gamma}, \quad (6)$$

along with the atomic Green function for site α ,

$$G^\alpha = G_0 + G_0 t^\alpha G_0. \quad (7)$$

In terms of these, the full Green function expanded about site α is

$$G = G^\alpha + G^\alpha T^{\alpha\alpha} G^\alpha \quad (8)$$

which can be manipulated into

$$G = G^\alpha + (1 + G_0 t^\alpha) (t^\alpha)^{-1} (\tau^{\alpha\alpha} - t^\alpha) (t^\alpha)^{-1} (1 + t^\alpha G_0) \quad (9)$$

which is the expression we use to determine G . Exploiting the two-dimensional translational symmetry $\tau^{\alpha\alpha}$, which sums all paths which start and end with a scattering event at site α , is found from an integral over the two-dimensional Brillouin zone (area Ω)

$$\tau^{\alpha\alpha} = \frac{1}{\Omega} \int_{\Omega} \tau^{\alpha\alpha}(\mathbf{k}_{\parallel}) d\mathbf{k}_{\parallel} \quad (10)$$

of the momentum-resolved scattering path operator. We evaluate $\tau^{\alpha\alpha}(\mathbf{k}_{\parallel})$ by summing paths taken by a wave with reduced momentum \mathbf{k}_{\parallel} beginning and ending at site α . This is done with the algorithms in Ref. [11]. $\tau^{\alpha\alpha}(\mathbf{k}_{\parallel})$ is evaluated for each site of interest. This is a relatively straightforward operation, but there is no longer the full separation between structure and potential which was one of the great advantages of conventional KKR theory. Nevertheless, the method is efficient, scaling linearly with the number of layers. Furthermore, by a layer doubling procedure we can also find the scattering matrices of semi-infinite half-spaces. Using these half-space scattering operators, layer scattering operators and the single atom scattering operator, t^α , we find the energy-resolved Green function for an atom in a layer embedded in a host crystal. The electronic properties can then be studied layer-resolved, via the LDOS which is defined as

$$\rho(\mathbf{r}, E) = \sum_i |\Psi_i(\mathbf{r})|^2 \delta(E - E_i) \quad (11)$$

in terms of the eigenstates i of the system, with energy E_i and wave function Ψ_i . This gives the charge density of states with energy E , and if necessary (as here) may be momentum resolved. In the Green function formulation it is given by

$$\rho(\mathbf{r}, E) = -\frac{1}{\pi} \text{Im} G(\mathbf{r}, \mathbf{r}, E + i\epsilon). \quad (12)$$

Thus we arrive at the LDOS for each atom in each layer.

In the work described in this paper we perform both interface and surface calculations. When performing a surface calculation we naturally divide the system into three regions: bulk, surface region including any overlayers, and vacuum. Each region is further divided into layers of atoms. We simulate the vacuum by empty spheres. The surface region consists of the overlayer structure which we want to study plus a number of substrate layers in which we expect changes in the electronic structure, due to the presence of the overlayer and the surface. For metallic systems this number can be quite small due to screening of the electronic perturbations, and

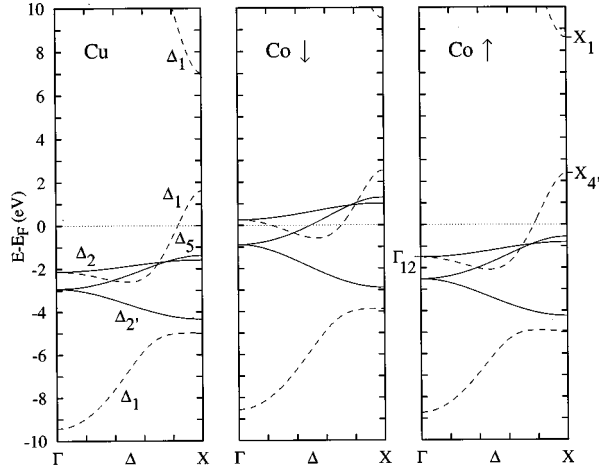


FIG. 1. Calculated band structures along ΓX of Cu, and fcc Co for both minority (\downarrow) and majority (\uparrow) spin electrons. We show bands with Δ_1 symmetry by a dashed line. The lattice parameter of Cu has been used for Co.

typically we use three. In our sandwich calculations the interlayer is enclosed by bulk on both sides. The rearrangement of charge occurring at the formation of surfaces and interfaces requires a self-consistent solution of the Schrödinger equation, by iterating on the potentials. In solving the Poisson equation we include both monopole and dipole contributions.¹⁵ In determining the charge and spin density we use 10 special \mathbf{k} points in the irreducible part of Ω , partial waves up to $\ell=3$ to calculate the scattering properties of each layer, and 21 plane waves in the layer coupling procedures.

III. RESULTS

We begin by presenting the band structure of Cu and fcc Co in Fig. 1, calculated using our computational method, and where the lattice parameter of Co has been taken as that of Cu. In fact fcc Co has a slightly smaller unit cell than Cu, so that small tetragonal distortions will arise in overlayers and sandwich structures synthesised from the two components. However, we are unable to determine these *ab initio*, and adopt the simpler procedure of using the Cu lattice parameter throughout.

We show the bands calculated along the Γ - Δ - X direction. These are the states which project on to the center of the surface Brillouin zone, $\bar{\Gamma}$, for structures which are assembled from a stacking of (001) planes, and are therefore the relevant states for understanding the quantum-well levels at $\bar{\Gamma}$. The most important band is that of Δ_1 symmetry (corresponding to states of s , p_z , and d_{z^2} orbitals), which crosses E_F in the case of Cu about 80% along ΓX . At X the V_{001} Fourier component of the potential opens up a gap extending between the $X_{4'}$ and X_1 levels, and at lower energies the Δ_1 band is crossed by the d -bands, some of which hybridize and result in complex dispersion.

In the following we restrict our attention to states with Δ_1 symmetry. Inspection of the band structure shows mismatch of the various Δ_1 bands in Cu and Co, giving rise to the possibility of discrete quantum-well states. In addition,

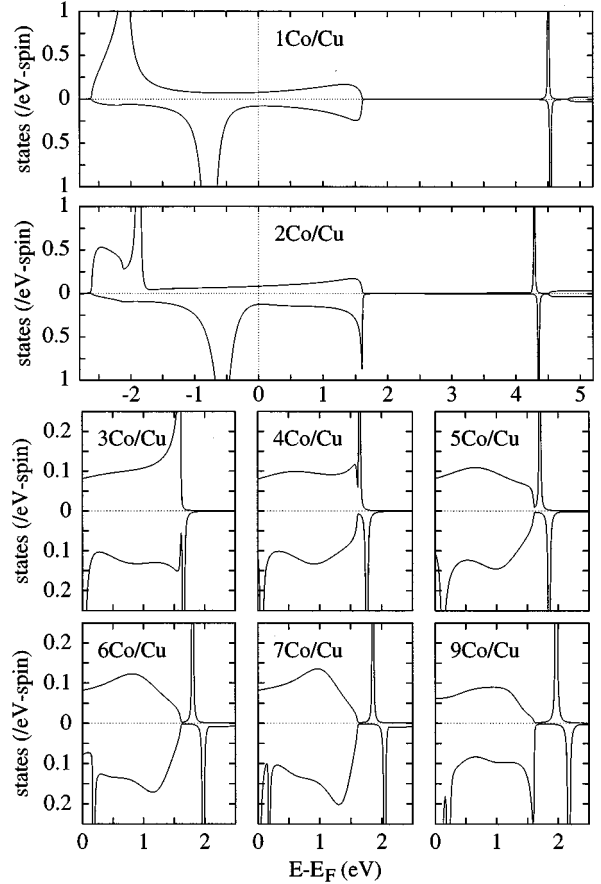


FIG. 2. Calculated local density of states with Δ_1 symmetry at $\bar{\Gamma}$ found in the surface Co layer of Co/Cu(001) overlayers of various thicknesses. For each plot the upper (lower) curve is of majority (minority) states.

the spin-polarized Co bands will result in spin-polarized Co states in Co thin films (as long as the Co remains magnetic) as well as spin-polarized Cu states in Cu thin films on account of the spin-dependent boundary conditions acting upon the electrons. Finally, the Co majority Γ_{12} - Δ_1 - $X_{4'}$ band closely resembles the corresponding Cu band, indicating that the Cu/Co interface will be more transparent to majority spin electrons than to minority spin electrons. We find below that this has a strong influence on the electronic structure.

A. Co/Cu(001) overlayers

Epitaxial growth of Co on Cu(001) has been reported^{16,17} for Co coverages up to 20 ML. From the bulk band structures in Fig. 1 we see that for this system discrete quantum-well levels may form in both spin channels, at energies between the Cu $X_{4'}$ level and the corresponding Co $X_{4'}$ level. Below these energies the Cu substrate is only partially reflective, so quantum well resonances will form.

In Fig. 2 we show the development of the LDOS of Δ_1 symmetry evaluated in the surface Co atomic spheres as the Co coverage increases. At 1 ML coverage the states are restricted to energies within the substrate continuum, with large contributions at energies corresponding to large LDOS in bulk Co, near the bottom of the respective spin-resolved band structures (we discuss the discrete states visible near

+4.5 eV below). At 2 ML coverage, a buildup of minority-spin states occurs near the upper edge ($X_{4'}$) of the substrate band, and at 3 ML coverage a discrete quantum-well state emerges from the continuum in the minority spin channel. The corresponding majority-spin level emerges at 4 ML coverage, and the spin-split pair disperse upwards in energy with increasing coverage. We find a splitting which increases from 0.12 eV at 4 ML to saturate around 0.19 eV above 8 ML coverage. This increase is a result of the increased localisation of the states within the ferromagnetic portion of the overlayer system as the Co coverage increases, reaching a natural limit which corresponds to the spin splitting of the associated band edges in bulk Co. Ortega *et al.*³ have observed the development of this quantum-well state in IPE measurements on Co/Cu(001), but quantitative comparison is not possible on account of the absence of spin resolution in their measurements and the limited energy resolution. Equally important, our calculations place the Cu $X_{4'}$ band edge at 1.65 eV, against the values observed in IPE (Ref. 3) of 1.8 eV, so that the state emerges at different energies in theory and experiment. We attribute this discrepancy to the use of the LDA for exchange correlation, although inaccuracies in our computational method will also contribute.

At 9 ML coverage we see the pattern beginning to repeat, with a buildup of states at the minority-spin band edge again visible, corresponding to a second discrete quantum-well level about to emerge (probably at 10 ML coverage, but we did not perform the calculation). The emergence of this state is preceded by a well defined peak in the LDOS, which moves towards the band edge as the coverage increases to 9 ML. This corresponds to a quantum-well resonance. Indeed, we observe structure (not shown) throughout the energy range where the Co bands overlap the Cu continuum, identifiable as quantum-well resonances. These resonances are generally narrower than those visible at higher energies, and their distribution rather complicated on account of the non-uniform dispersion of the Δ_1 band (Fig. 1).

The remaining significant feature in Fig. 2 is the discrete energy level visible near 4.5 eV shown in the 1 ML and 2 ML plots. We identify this as a surface state, and furthermore as a barrier-induced surface state.^{18,19} We make this identification based upon the observation that by far the largest weight of the wave function is to be found in the two layers above the surface, and not within the crystal. Therefore, the state is related to the image states which would be present if we used a long-ranged image potential, and indeed the energy, about 0.5 eV below the vacuum level, is similar to the energies of image states observed by inverse photoemission.²⁰ Our short-ranged LDA potential can only bind one such level, as against the infinite Rydberg series obtained from the actual image potential. As expected of image states, the energy closely follows the vacuum level. We find it at 4.5, 4.3, and 4.4 eV for 1 ML, 2 ML, and 3 ML overlayers, respectively, for which our calculated work functions are 5.15, 4.83, and 4.93 eV.^{21–23} Of particular interest is the splitting of the image state, which we find to be 30 meV for 1 ML Co/Cu(001), rising to 60 meV for 2 ML coverage and above. This splitting is comparable to that found for the Fe(110) image state (55 meV for the lowest image state²⁴), despite the lower moment of the surface atom here (reduced by over 30%) and the obvious difference that we have a

ferromagnetic thin film rather than an extended crystal. Clearly, ferromagnetic thin films offer a potential route towards maximally spin-split image states, in addition to previously suggestions of crystal orientation and adsorbate-induced work function modification.²⁵

Finally, for this system, we find a surface Co moment of $1.84 \pm 0.01 \mu_B$ for all coverages, an enhancement of 10% over the bulk value (our bulk value of $1.68 \mu_B$ is slightly greater than the $1.64 \mu_B$ found at the true Co lattice spacing). This compares with the 12% enhancement found by Aldén *et al.*²⁷ for the Co(001) surface, and 13% enhancement found by Li *et al.*²⁶ for the muffin-tin moment in a seven layer full-potential slab calculation.

B. Cu/Co(001) overlayers

Quantum-well states near E_F in the Cu/Co overlayer system are very different from those in the Co/Cu system. Inspection of the band structures (Fig. 1) shows that in this case the substrate bands at $\bar{\Gamma}$ are spin polarized, and that the Cu overlayer Δ_1 band edge ($X_{4'}$) lies *below* both the Co substrate band edges, so that Cu Δ_1 states do not lie in a substrate band gap. However, the Cu Δ_1 band extends below the corresponding substrate bands, giving rise to the possibility of discrete quantum-well levels at lower energies. These can occur at energies below -2.08 eV for majority spin and -0.58 eV for minority spin electrons.

In Fig. 3 we plot the calculated LDOS found in the surface Cu layer of Cu/Co(001) films of 1–9 ML coverage. Again we only consider states of Δ_1 symmetry at $\bar{\Gamma}$. The flat portion of the Cu $\Gamma_{12}-\Delta_1-X_{4'}$ band (Fig. 1) gives rise to a large number of quantum-well levels at energies below -2 eV. At higher energies the bulk Cu band disperses more rapidly upwards and the corresponding quantum-well states are more widely distributed, remaining as discrete states clearly visible in the minority-spin channel, but immediately merging with the substrate continuum in the majority spin channel and losing their integrity.

As a function of Cu coverage the minority spin quantum well levels are seen to disperse smoothly upwards in energy, and it is possible to observe the transition from discrete level to resonance. For example, a discrete spin level seen at -1.5 eV at 2 ML coverage may be followed upwards in energy, appearing at -1.0 and -0.7 eV at 3 ML and 4 ML coverage, respectively. At 5 ML the level has just entered the continuum energy range, appearing as a strong feature near -0.5 eV, which then continues to rise in energy, appearing as a local maximum in the LDOS near -0.1 , $+0.2$, $+0.5$, and $+0.6$ eV at 6, 7, 8, and 9 ML coverage. Counting down in energy this is the second quantum-well level, the first being a broad resonance at about $+1$ eV. The third appears at -1.7 eV at 5 ML coverage and follows a similar evolution with increasing coverage.

In the top panel of Fig. 4 we plot the energies of the minority spin quantum-well levels obtained from our calculations as a function of Cu thickness, and we compare them with the energies extracted from spin-resolved PE experiments performed by Carbone *et al.*⁴ There is very good agreement, especially for the third level. The lower panels show the spin-integrated LDOS and the spin polarization, both of which have been calculated at E_F . These are given

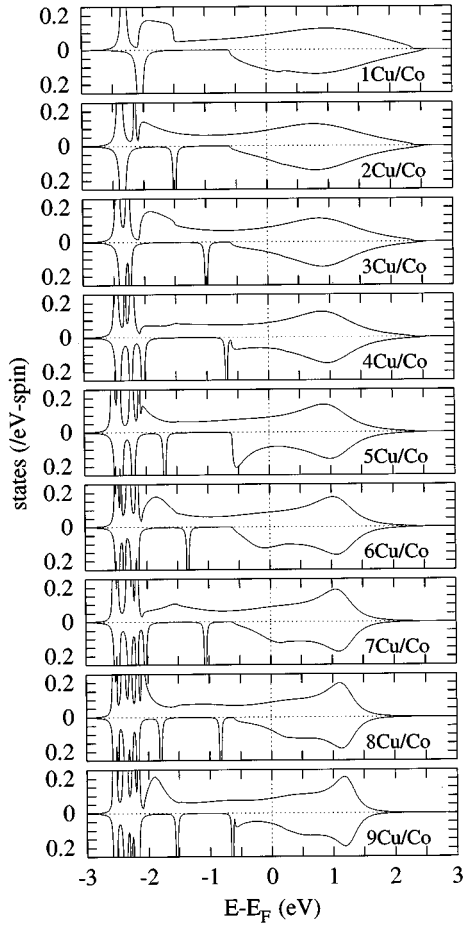


FIG. 3. Calculated local density of states with Δ_1 symmetry at $\bar{\Gamma}$ found in the surface Cu layer of Cu/Co(001) overlayers of various thicknesses. For each plot the upper (lower) curve is of majority (minority) states. The cusps seen near $+0.25$ eV in the minority spin LDOS and -1.5 eV in the majority spin LDOS at various coverages result from the Co substrate Γ_{12} band edge.

for the surface Cu layer, the central Cu layer, and the overlayer average, and all exhibit strong variation with Cu thickness. In particular they oscillate in a similar manner to the intensity and polarization of the PE signal measured by Carbone *et al.*⁴ (A more sophisticated comparison would take into account contributions from deeper layers, background contributions to the PE signal and also the energy resolution of the experiment.) In particular, we obtain a similar period, of about 6 ML, and we also find the polarization is a maximum when the intensity is at a minimum. This latter result occurs because the variation in the LDOS at E_F arises almost exclusively in the minority-spin channel, so that the intensity peaks whenever a minority spin quantum-well resonance passes through E_F , which also causes a large negative polarization. Indeed, inspection of Fig. 3 shows that in the energy range from -1.5 eV to E_F there are no majority-spin features in the LDOS to speak of. The resonances are so broad as to be indistinguishable. In this we are more in agreement with the finding of Garrison *et al.*,⁵ who concluded only minority spin features existed, than Carbone *et al.*,⁴ who identified majority-spin features in their spin-resolved PE measurements. (We are also unable to identify features in the LDOS of subsurface Cu layers which could be respon-

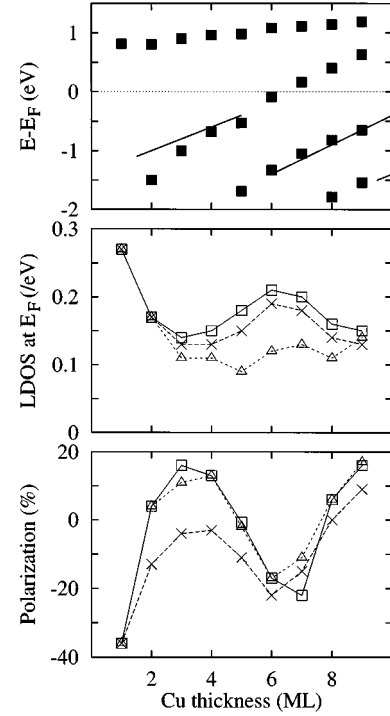


FIG. 4. Top: Minority-spin quantum well energy levels in Cu/Co(001) as a function of Cu coverage. Symbols show the calculated values, and the lines the experimental dispersions measured by Carbone *et al.* (Ref. 4). Middle: Calculated local density of states (majority+minority) in the Cu/Co(001) overlayer evaluated at the Fermi energy, as a function of Cu coverage. Squares, topmost Cu layer; triangles, central Cu layer; crosses, average throughout the Cu layers. Bottom: spin polarization of states at $\bar{\Gamma}$ and at the Fermi energy in the Cu/Co(001) overlayer, as a function of Cu coverage. Symbols are the same as in the middle panel.

sible.) This difference in behavior between the two spin channels is consistent with the greater degree of similarity that exists between the Cu bands and those of the Co majority states, as against the Co minority spin states, which results in a more transparent interface for majority spin electrons and therefore less confinement.

C. Co/Cu/Co(001) sandwiches

We now consider the Co/Cu/Co(001) sandwich, which naturally has the same substrate continuum energy ranges as the Cu/Co(001) overlayer. For this system we have performed a true interface calculation, with semi-infinite Co half-spaces sandwiching a Cu film, and we have forced the Co substrates to be ferromagnetically aligned.

In Fig. 5 we show the LDOS in the central Cu layer for several Cu thicknesses, again considering states at $\bar{\Gamma}$ of Δ_1 symmetry. A dense distribution of discrete levels at energies between -3 and -2 eV again results from the flat portion of the Cu $\Gamma_{12}-\Delta_1-X_4'$ band, as in the overlayer case, and with increasing film thickness states with minority spin disperse upwards. Indeed, above 2 ML coverage there is very good agreement between the locations of the discrete levels found in overlayers and sandwiches of the same Cu thickness. The poorer agreement in the thinnest films is probably due to the influence of interfacial bonding.

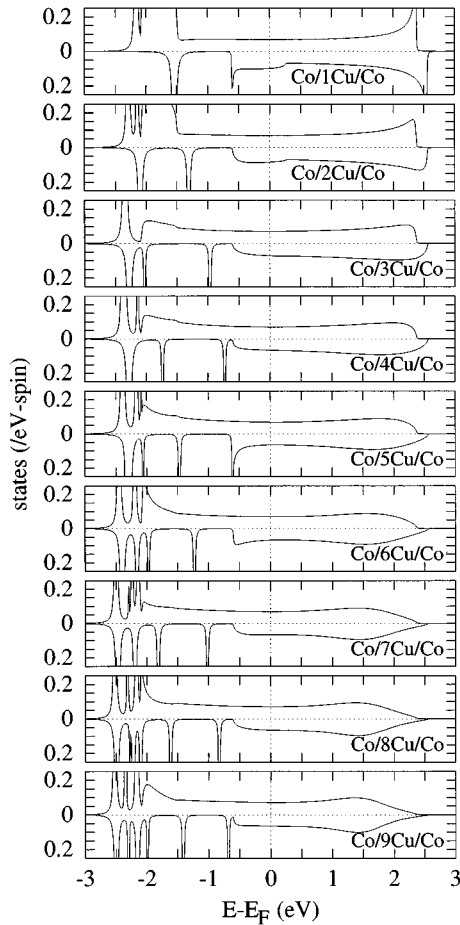


FIG. 5. Calculated local density of states with Δ_1 symmetry at $\bar{\Gamma}$ found in the central Cu layer of Co/Cu/Co(001) sandwiches of various thicknesses. For each plot the upper (lower) curve is of majority (minority) states.

Following the minority spin quantum-well level which is at -1 eV for 3 ML Cu, we find it just enters the continuum at 5 ML, forming a strong feature at the band edge. However with further increases of the Cu thickness it is not possible to follow this level in the form of a resonance—unlike in the overlayer, the coupling to the substrate is sufficiently strong to destroy all vestiges of the state. In Fig. 6 we show that this is not a consequence of directing attention at the central plane of the sandwich, showing the LDOS and polarization at E_F on the central Cu layer, the interfacial Cu layer and also the sandwich average. The strong variations with Cu thickness which were evident in the overlayer are no longer present in the sandwich.

Our viewpoint for interpreting the sandwich electronic structure is not unique. As an alternative one can determine a difference LDOS, to highlight the change in states induced by the interacting half-spaces.^{6,10} However, we choose to consider a quantum-well state as a property of the sandwich alone, not a result of some difference procedure, so that the integrity of the resonance should be sufficient for it to be identifiable within the electronic structure of the sandwich. In this regard we apply the same criteria as would be applied in interpreting PE or IPE measurements. Differences tend to exhibit oscillatory structure (Fig. 1 in Ref. 6, for example) which, whilst exhibiting peaks which may be interpreted as

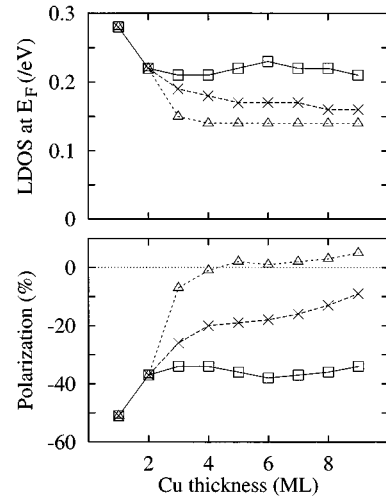


FIG. 6. Local density of states (top) and spin polarization (bottom) of states at $\bar{\Gamma}$ at the Fermi energy in Co/Cu/Co(001) sandwiches, as a function of Cu thickness. Squares, interfacial Cu layer; triangles, central Cu layer; crosses, average throughout the Cu layers.

resonances, also yield “negative” features of comparable magnitude yet which have no sensible physical interpretation.

Examining in more detail the quantum well states we find interesting behavior in the layer-projected orbital contributions. The Δ_1 states are built from s , p_z , and d_{z^2} orbital contributions, and these shown are in Fig. 7 for the minority spin level found at -1.4 eV in the 9 ML Co/Cu/Co(001) sandwich. At the Co/Cu interface we find large d_{z^2} contributions on both the interfacial planes, evidence of strong hybridization with the highly polarized Co d bands. The s and p_z contributions at the interface are much weaker. Within the Cu interlayer the total density associated with the quantum-well level is relatively constant, but this masks considerable variation in orbital composition on the different Cu planes. These oscillate with a period of approximately 4 ML, the s and d_{z^2} contributions varying in phase but reaching a maxi-

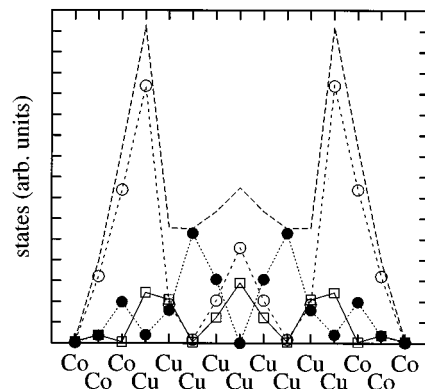


FIG. 7. Layer-projected orbital contributions to the minority spin Δ_1 quantum-well level at -1.4 eV in the Co/Cu/Co(001) sandwich with 9 ML Cu. Squares: s ; filled circles: p_z ; open circles: d_{z^2} . The lines are to guide the eye. The upper line is the sum $s + p_z + d_{z^2}$.

mum (minimum) when the p_z contribution is a minimum (maximum). The s and p_z contributions are larger away from the interface, so that within the interlayer the three orbital components are comparable. The sizeable d_{z^2} contribution shows that, at least below -1 eV, the quantum-well levels cannot be considered to be sp -like free electron states.

IV. DISCUSSION

We find substantial agreement between the results of our *ab initio* calculations of quantum-well states in Co/Cu(001) and Cu/Co(001) overlayers and various spectroscopy studies on corresponding systems. In the case of Cu/Co(001) we confirm the formation of a strongly thickness dependent electronic structure within the Cu overlayer. The nature of the electronic states may be broadly predicted from the bulk band structures. Thus overlayer states occur at energies that coincide with the ranges of the Cu bulk bands, the states appearing as discrete levels in the regions of substrate band gaps and resonances where substrate states exist. Near E_F this results in an oscillatory local density of states and net spin polarization, primarily as a result of the formation of minority-spin quantum-well resonances which exhibit regular dispersion, passing through E_F approximately every 6 ML. In the majority spin channel the electronic structure near E_F shows much weaker dependence on film thickness. This reflects the similarity between the majority spin Δ_1 Co band and the corresponding Cu band, resulting in a largely transparent interface and poor confinement. Even in the minority spin channel the resonances have a considerable width. When a similar study is made of the Co/Cu/Co(001) multilayer system, we find a distribution of discrete levels which is closely related to those found in the Cu/Co(001) overlayer, but that there is little evidence of quantum-well resonances at energies near E_F in either spin channel. In this system there is no evidence of a strongly thickness dependent electronic structure in states near E_F .

These findings are not difficult to rationalize. At energies within substrate band gaps Cu electrons traveling towards the substrate undergo complete reflection. At energies below the vacuum level, electrons in a Cu overlayer also undergo complete reflection at the Cu/vacuum interface. This similarity in the scattering at the two different interfaces leads to

comparable distributions of discrete quantum-well states in the overlayer and sandwich geometries. Conversely, at energies which coincide with a Co bulk band, electrons travelling toward the substrate only undergo partial reflection. In this case the electrons are only partially confined, resulting in resonant energy levels with finite widths. Under these circumstances there is a large difference between being partially confined on one side of the thin film but completely confined on the other, as in an overlayer, and only being confined partially only both sides, as in the sandwich. The latter results in less localisation to the thin film, and consequently larger resonance widths and a weaker thickness dependent electronic structure.

This is clearly a simplification. At a band gap an electron picks up a phase upon reflection from the substrate which will, in general, differ from the phase picked up from reflection at the vacuum barrier, and this can result in shifts in confined energy levels.²⁸ Similarly, the extent to which resonances are broadened and the level structure “washed out” depends upon the actual reflectivity at the substrate interface, which varies with energy across a substrate band.²⁹ In this regard, more detailed experimental investigations of the resonance widths of quantum-well features in overlayers would be very useful. It should also be stressed that the weakness of quantum-well effects at the Fermi energy which we find here in the Co/Cu/Co sandwich structures does not necessarily imply that they are unimportant for determining magnetic coupling—theories of the interlayer coupling indicate that asymptotically the interaction is governed by states at E_F , and that the long period interaction does originate from $\bar{\Gamma}$ states. However, in general our results indicate that one should be careful in extrapolating the nature of the electronic structure measured or calculated in overlayer systems, to that present in related modulated structures.

ACKNOWLEDGMENTS

We have had useful discussions with Jeroen van Hoof and Theo Rasing. The work was supported by Stichting FOM (J.E.I.) and also by the Human Capital and Mobility Network “*Ab initio* (from electronic structure) calculation of complex processes in materials” (Contract No. ERB-CHRXCT930369).

*Present address: Department of Physics and Astronomy, University of Wales, College of Cardiff, P.O. Box 913, Cardiff CF2 3YB, Great Britain.

¹M. van Schilfgaarde and W.A. Harrison, Phys. Rev. Lett. **71**, 3870 (1993).

²J.E. Ortega and F.J. Himpsel, Phys. Rev. Lett. **69**, 844 (1992).

³J.E. Ortega, F.J. Himpsel, G.J. Mankey, and R.F. Willis, Phys. Rev. B **47**, 1540 (1993).

⁴C. Carbone, E. Vescovo, O. Rader, W. Gudat, and W. Eberhardt, Phys. Rev. Lett. **71**, 2805 (1993).

⁵K. Garrison, Y. Chang, and P.D. Johnson, Phys. Rev. Lett. **71**, 2801 (1993).

⁶L. Nordström, P. Lang, R. Zeller, and P.H. Dederichs, Europhys. Lett. **29** (5), 395 (1995).

⁷P. Bruno and C. Chappert, Phys. Rev. Lett. **67**, 1602 (1991).

⁸M.T. Johnson, S.T. Purcell, N.W. McGee, R. Coehoorn, J. van de

Stegge, and W. Hoving, Phys. Rev. Lett. **68**, 2688 (1992).

⁹B.A. Jones and C.B. Hanna, Phys. Rev. Lett. **71**, 4253 (1992).

¹⁰J. Mathon, M. Villeret, R.B. Muniz, J. d’Albuquerque e Castro, and D.M. Edwards, Phys. Rev. Lett. **74**, 3696 (1995).

¹¹J.M. MacLaren, S. Crampin, D.D. Vvedensky, and J.B. Pendry, Phys. Rev. B **40**, 12 164 (1989).

¹²S. Crampin, J. Phys. Condens. Matter **5**, 4647 (1993).

¹³J. Korringa, Physica **13**, 392 (1947); W. Kohn and N. Rostoker, Phys. Rev. **94**, 1111 (1954).

¹⁴A. Gonis, *Green’s functions for ordered and disordered systems* (North-Holland, Amsterdam, 1992).

¹⁵H.L. Skriver and N.M. Rosengaard, Phys. Rev. B **43**, 9538 (1991).

¹⁶A. Clarke, G. Jennings, R.F. Willis, P.J. Rous, and J.B. Pendry, Surf. Sci. **187**, 327 (1987).

¹⁷C.M. Schneider, P. Bressler, P. Schuster, J. Kirschner, J.J. de

- Miguel, and R. Miranda, Phys. Rev. Lett. **64**, 1059 (1990).
- ¹⁸P.M. Echenique and J.B. Pendry, J. Phys. C **11**, 2065 (1978).
- ¹⁹Similar states have been observed in other LDA surface studies, e.g., F. Ciccacci, S. De Rossi, A. Taglia, and S. Crampin, J. Phys. Condens. Matter **6**, 7227 (1994).
- ²⁰D. Straub and F.J. Himpsel, Phys. Rev. B **33**, 2256 (1986).
- ²¹We are only aware of a measurement of the fcc Co work function of a polycrystalline sample, of 5.0 eV (Ref. 22). For a discussion of the accuracy of the calculated work functions see Ref. 23. We expect the relative workfunctions to be more accurate than the absolute values.
- ²²H.B. Michaelson, J. Appl. Phys. **48**, 4729 (1977).
- ²³S. Crampin, Phys. Rev. B **49**, 14 035 (1994).
- ²⁴M. Nekovee, S. Crampin, and J.E. Inglesfield, Phys. Rev. Lett. **70**, 3099 (1993).
- ²⁵F.J. Himpsel, Phys. Rev. B **43**, 13 394 (1991).
- ²⁶Chun Li, A.J. Freeman, and C.L. Fu, J. Magn. Magn. Mater. **75**, 53 (1988).
- ²⁷M. Aldén, S. Mirbt, H.L. Skriver, N.M. Rosengaard, and B. Johansson, Phys. Rev. B **46**, 6303 (1992).
- ²⁸N.V. Smith, N.B. Brookes, Y. Chang, and P.D. Johnson, Phys. Rev. B **49**, 332 (1994).
- ²⁹S. Crampin, S. De Rossi, and F. Ciccacci, Phys. Rev. B (to be published).